Identification of Sequences in Apolipoprotein(a) that Maintain Its Closed Conformation: A Novel Role for Apo(a) Isoform Size in Determining the Efficiency of Covalent Lp(a) Formation†

Lev Becker, P. Michael Cook, and Marlys L. Koschinsky*

Department of Biochemistry, Queen's University, Kingston, Ontario, Canada, K7L 3N6

Received March 8, 2004; Revised Manuscript Received May 4, 2004

ABSTRACT: We have previously demonstrated that, in the presence of the lysine analogue ϵ-aminocaproic acid, apolipoprotein(a) [apo(a)] undergoes a conformational change from a closed to an open structure that is characterized by a change in tryptophan fluorescence, an increase in the radius of gyration, an alteration of domain stability, and an enhancement in the efficiency of covalent lipoprotein(a) [Lp(a)] formation. In the present study, to identify sequences within apo(a) that maintain its closed conformation, we used ϵ-aminocaproic acid to probe the conformational status of a variety of recombinant apo(a) isoforms using analytical ultracentrifugation, differential scanning calorimetry, intrinsic fluorescence, and in vitro covalent Lp(a) formation assays. We observed that the closed conformation of apo(a) is maintained by intramolecular interaction(s) between sequences within the amino- and carboxyl-terminal halves of the molecule. Using site-directed mutagenesis, we have identified the strong lysine-binding site present within apo(a) kringle IV type 10 as an important site within the C-terminal half of the molecule, which is involved in maintaining the closed conformation of apo(a). Apo(a) exhibits marked isoform size heterogeneity because of the presence of varying numbers of copies of the kringle IV type-2 domain located within the amino-terminal half of the molecule. Using recombinant apo(a) species containing either 1, 3, or 8 copies of kringle IV type 2, we observed that, while apo(a) isoform size does not alter the affinity of apo(a) for low-density lipoprotein, it affects the conformational status of the protein and therefore influences the efficiency of covalent Lp(a) assembly. The inverse relationship between apo(a) isoform size and the efficiency of covalent Lp(a) formation that we report in vitro may contribute to the inverse relationship between apo(a) isoform size and plasma Lp(a) concentrations that has been observed in vivo.

Elevated plasma levels of lipoprotein(a) [Lp(a)][1] have been identified as a risk factor for the development of vascular diseases (reviewed in refs *1* and *2*). Lp(a) contains a low-density lipoprotein (LDL)-like moiety as well as a unique glycoprotein component termed apolipoprotein(a) [apo(a)]. In the context of the Lp(a) particle, the apolipoproteinB-100 (apoB-100) component of the LDL-like moiety is linked to apo(a) by a single disulfide bridge (*3*, *4*). Apo(a) contains contiguous repeats of a sequence that resembles plasminogen kringle IV, followed by sequences that are highly homologous to the kringle V and protease domains of plasminogen (*5*). The kringle IV domains of apo(a) are classified into 10 distinct subclasses; the kringle IV type-2 domain (KIV_2) is present in variable copy number, which forms the molecular basis for the observed isoform size heterogeneity of Lp(a) (*6*, *7*). Apo(a) isoforms ranging from 3 to greater than 40 copies of KIV_2 have been identified in the human population (*8*). A general inverse relationship between apo(a) isoform size and plasma Lp(a) concentrations has been reported (*9*), thereby establishing a genetic basis for the determination of plasma Lp(a) levels. One reported explanation for this inverse correlation is the reduced secretion efficiency of larger apo(a) isoforms, leading to their increased intracellular degradation (*10*).

Some of the apo(a) kringle IV domains are characterized by the presence of lysine-binding pockets. Apo(a) KIV types 5−8 (KIV_{5-8}) each contain a weak lysine-binding site (WLBS) (*11*, *12*), while apo(a) kringle IV type 10 (KIV_{10}) contains a stronger lysine-binding site (SLBS) that has been proposed to mediate the binding of apo(a)/Lp(a) to ligands such as fibrin (*13*−*15*). Lp(a) assembly is a two-step process in which initial noncovalent interactions between apo(a) and apoB-100 precede the formation of a single disulfide bond (*11*, *12*, *16*). The noncovalent step is mediated by interactions between the WLBS present within apo(a) KIV_{7-8} (*18*) and lysine residues (K680 and K690) within the amino-terminal 18% (apoB-18) of apoB-100 (*19*, *20*). As such, lysine and lysine analogues such as ϵ-aminocaproic acid (ϵ-ACA) are potent inhibitors of the noncovalent interaction between apo(a) and apoB-100 and accordingly reduce the efficiency of covalent Lp(a) formation (*12*, *17*).

† This work was supported by a grant (11271) from the Canadian Institutes of Health Research (to M.L.K.). M.L.K. is a Career Investigator of the Heart and Stroke Foundation of Ontario.

* To whom correspondence should be addressed: Department of Biochemistry, Queen's University, Kingston, Ontario, Canada K7L 3N6. Telephone: (613) 533-6586. Fax: (613) 533-2987. E-mail: mk11@post.queensu.ca.

[1] Abbreviations: Lp(a), lipoprotein(a), LDL, low-density lipoprotein; apo(a), apolipoprotein(a); apoB, apolipoproteinB; ϵ-ACA, ϵ-aminocaproic acid; HBS, HEPES-buffered saline; WLBS, weak lysine-binding site; SLBS, strong lysine-binding site; CM, conditioned medium; AUC, analytical ultracentifugation; DSC, differential scanning calorimetry.

10.1021/bi049536d CCC: $27.50
Published on Web 07/17/2004

We have recently demonstrated that the conformational status of apo(a) plays a significant role in determining the efficiency of covalent Lp(a) particle formation (*21*). Uncomplexed apo(a) exists in a "closed" conformation that is stabilized by interdomain interactions. The addition of ϵ-ACA elicits a substantial conformational change in apo(a) to an "open" structure. Apo(a), in the open conformation, forms covalent Lp(a) particles approximately 6 times more efficiently than the closed form of the molecule. As such, we observed that the addition of ϵ-ACA resulted in a complex, biphasic effect on covalent Lp(a) assembly, whereby low concentrations promote assembly by altering the conformation of apo(a), while higher concentrations of this ligand attenuate the process by inhibiting noncovalent interactions between apo(a) and LDL (*21*). These data suggest that the efficiency of covalent Lp(a) assembly can be regulated by sequences that do not directly participate in the noncovalent step of Lp(a) assembly but rather maintain the closed conformation of apo(a) (*21*).

In the present study, we examined the physical properties of different recombinant apo(a) variants using a variety of biophysical techniques with the goal of identifying sequences responsible for maintaining the closed conformation. We further assessed the effect of apo(a) isoform size on the conformation of apo(a) as well as the efficiency of both noncovalent and covalent Lp(a) assembly. Our data demonstrate that the number of copies of the KIV_2 domain in apo(a) has a profound influence on the efficiency of the covalent step of Lp(a) assembly. This represents a novel mechanism, which may contribute to the inverse correlation that has been reported between apo(a) isoform size and plasma Lp(a) concentrations in the human population.

EXPERIMENTAL PROCEDURES

Expression and Purification of Recombinant Apo(a) Variants. All of the recombinant apo(a) [r-apo(a)] variants used, with the exception of apo(a) KIV_{1-4}, were cloned and stably expressed in human embryonic kidney (HEK) 293 cells as previously described (*22*−*24*). An expression plasmid encoding the KIV_{1-4} r-apo(a) variant was generated using the parental 17-kringle (17K) r-apo(a) expression plasmid pRK5ha17 (*22*). Briefly, the KIV_{1-4}-encoding construct was generated using an *Eco*RI/*Sma*I fragment derived from pRKha17 (containing sequences encoding the 5′-untranslated and signal sequences followed by KIV_1, eight copies of KIV_2, KIV_3, and KIV_4) and an *Eco*RV/*Eco*RI fragment (containing sequences encoding a stop codon engineered between the kringle V and protease-like domains). These fragments were used for a 3-part ligation into pRKha17, which had been digested with *Eco*RI to remove the 17K apo(a) sequence; the resultant vector was designated pRK5haKIV$_{1-4}$. This expression plasmid was used to generate a stably expressing HEK 293 cell line as previously described (*22*).

With the exception of apo(a) KIV_{1-4}, all of the r-apo(a) variants were purified from the conditioned media (CM) of stably expressing cell lines using lysine-Sepharose (Amersham Biosciences) affinity chromatography as previously described (*22*, *23*). For the purification of apo(a) KIV_{1-4}, CM containing the recombinant protein was passed over a 20-mL lectin-Sepharose (Amersham Biosciences) column. The column was washed with HEPES-buffered saline (HBS; 20 mM HEPES at pH 7.4 and 150 mM NaCl) containing 1 M NaCl, and bound proteins were eluted by the addition of HBS containing 1 M NaCl and 0.5 M *N*-acetyl-D-glucosamine (Sigma−Aldrich). KIV_{1-4}-containing fractions were pooled, dialyzed extensively against 20 mM Tris-HCl at pH 8.0, and applied to a 5-mL Q-Sepharose (Amersham Biosciences) column. Bound proteins were eluted with a continuous salt gradient from 0 to 0.6 M NaCl (80-mL total gradient volume). Apo(a) KIV_{1-4} eluted between 350 and 600 mM NaCl. These fractions were pooled, dialyzed extensively against 20 mM HEPES at pH 7.4, and applied to a 5-mL Heparin-agarose (Sigma−Aldrich) column. The flow through was collected, dialyzed against HBS, and concentrated using poly(ethylene glycol) (PEG) 20000 (Fluka). The final protein concentration was determined by measuring absorbance at 280 nm (with correction for Rayleigh light scattering) using a calculated extinction coefficient ($E_{0.1\%} = 1.63$) (*25*). Protein purity was assessed by SDS−PAGE followed by Coomassie blue staining.

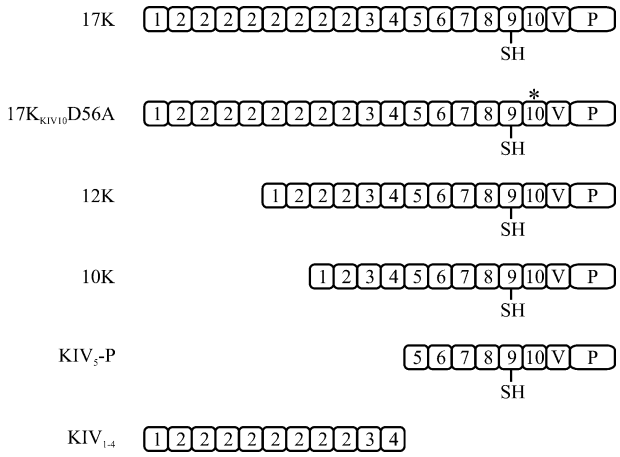

FIGURE 1: Recombinant apo(a) variants used in this study. Recombinant apo(a) variants corresponding to 17K, 17K$_{KIV10}$D56A, 12K, 10K, KIV_{1-4}, and KIV_5-P were constructed in the pRK5 vector and expressed in human embryonic kidney 293 cells as outlined in the Experimental Procedures. 17K$_{KIV10}$D56A contains an Asp to Ala substitution at amino acid position 56 of KIV_{10} that disrupts the SLBS.

Measurements of Intrinsic Fluorescence. Intrinsic fluorescence measurements of r-apo(a) were performed using an LS50B luminescence spectrometer (Perkin−Elmer Life Sciences) as previously described (*21*). Briefly, 70 nM each of 17K$_{KIV10}$D56A (a variant containing an amino acid substitution that disrupts the SLBS in KIV_{10}) (*24*), 17K, as well as KIV_5-P [corresponding to the carboxyl-terminal half of apo(a)] and KIV_{1-4} r-apo(a) [corresponding to the amino-terminal half of apo(a)] (Figure 1) was titrated with a range of ϵ-ACA concentrations (from 41 μM to 216 mM). For the simultaneous titration of KIV_{1-4} and KIV_5-P, both proteins were added to a final concentration of 70 nM in the same cuvette. Resultant fluorescence changes were subjected to nonlinear regression analysis using equilibrium equations describing one or two binding sites for ϵ-ACA as appropriate. The fractional fluorescence (I/I_o) obtained for either the 17K or 17K$_{KIV10}$D56A r-apo(a) variants was subtracted from the changes in the corresponding I/I_o values [$\Delta(I/I_o)$] obtained for the simultaneous titration of KIV_{1-4} and KIV_5-P. The excess fluorescence changes obtained were modeled according to simple hyperbolic equations to obtain the maximal

fractional fluorescence changes and the $K_{D(app)}$ values for the intramolecular interactions in 17K and 17K_{KIV10}D56A r-apo(a).

Analytical Ultracentrifugation of Recombinant Apo(a). Sedimentation experiments were performed using a Beckman XL-I analytical ultracentrifuge as previously described (*21*). Briefly, sedimentation velocity experiments were performed at a constant temperature (20 °C) using a rotor speed of 22 500 rpm for 17K_{KIV10}D56A, 25 000 rpm for 10K and 12K, and 30 000 rpm for KIV_5-P and KIV_{1-4}. For some r-apo(a) variants, the dependence of $\Delta S_{w,20}$ on the concentration of ϵ-ACA was modeled by regression of the data according to a simple hyperbolic relationship.

Differential Scanning Calorimetry (DSC). DSC experiments were conducted using a VP-DSC calorimeter (Microcal) as previously described (*21*). For the third thermal transition of 12K r-apo(a), the dependence of the ΔH^*_{mIII}:ΔH_{mIII} ratio (corresponding to the temperature-independent van't Hoff and calorimetric heat changes, respectively) on the concentration of ϵ-ACA was modeled according to a simple hyperbolic relationship.

Purification and Modification of LDL with 5′-Iodoacetamido-fluorescein. LDL was purified from human plasma and labeled with 5′-iodoacetamido-fluorescein as previously described (*21*). The concentrations of LDL and fluorescently labeled LDL (flu-LDL) were determined using a modified Bradford assay, and the preparations were stored at 4 °C for no longer than 3 days prior to use.

Binding of Recombinant Apo(a) to flu-LDL. Fluorescein fluorescence measurements demonstrating r-apo(a) binding to flu-LDL were performed using an LS50B luminescence spectrometer (Perkin−Elmer Life Sciences) as previously described (*21*). Briefly, flu-LDL (50 nM) was titrated with either 17K_{KIV10}D56A, 12K, or 10K r-apo(a). The resultant fluorescence changes were subjected to nonlinear regression using the following quadratic equation:

$$\Delta I = 0.5dI(K_D + [A]_0 + [B]_0 - \sqrt{(K_D + [A]_0 + [B]_0)^2 - 4[A]_0[B]_0}) \quad (1)$$

where ΔI is the measured fluorescence change, dI is the difference between the fluorescence coefficient for LDL in the free and the apo(a)-bound states, K_D is the dissociation constant for the flu-LDL:apo(a) interaction, and $[A]_0$ and $[B]_0$ are the total concentrations of r-apo(a) and flu-LDL, respectively.

Transient Transfection and Metabolic Labeling of r-apo(a) with [^{35}S]cysteine. Transient transfection of 17K, 17K_{KIV10}D56A, 12K, and 10K r-apo(a) into HEK 293 cells and metabolic labeling with [^{35}S]cysteine (Perkin−Elmer Life Sciences) was performed as previously described (*21*). The concentration of [^{35}S]cysteine-labeled apo(a) was determined by ELISA using purified apo(a) as a standard, and the labeled proteins were stored in aliquots at −70 °C prior to use.

Covalent Lp(a) Assembly Assays. In vitro covalent Lp(a) assembly assays were performed essentially as previously described (*21*). Purified native LDL (50 nM) was incubated with CM containing 4 nM [^{35}S]cysteine-labeled 17K_{KIV10}D56A, 12K, or 10K r-apo(a), in the presence of a wide range of ϵ-ACA concentrations (0, 1 μM, 10 μM, 100 μM, 1 mM, 5 mM, 10 mM, 25 mM, and 100 mM), at 37 °C in a total reaction volume of 50 μL. For the 10K and 12K r-apo(a) variants, ϵ-ACA titrations were conducted at LDL concentrations of 12.5, 25, and 50 nM; for 17K_{KIV10}D56A, LDL concentrations of 12.5, 25, 50, and 75 nM were used. After incubation for 4 h, the reactions were stopped by the addition of an equal volume of 2X Laemmli sample buffer (*26*) in the absence of a reducing agent and heated at 95 °C for 5 min. Samples were then subjected to SDS−PAGE on 4% polyacrylamide gels. The gels were placed in fixing solution for 20 min, followed by incubation in Amplify solution (Amersham Biosciences) for 30 min. The gels were then dried and exposed onto an Imaging Screen (BioRad) for 16 h. The screen was developed using a Biorad Molecular Imager FX, and the bands were quantified using Quantity One 4.0.1 densitometry software. The extent of r-Lp(a) particle formation was calculated to be the density of the Lp(a) band divided by the sum of the densities of the Lp(a) and apo(a) bands, multiplied by 100. The initial rate of covalent Lp(a) assembly (V_0) was estimated by dividing the amount of Lp(a) formed (in nanomolars) by the incubation time. For 17K_{KIV10}D56A, the initial rate of covalent Lp(a) assembly in the absence of ϵ-ACA was modeled with respect to the concentration of LDL using the hyperbolic relationship shown below (Scheme 1).

Scheme 1

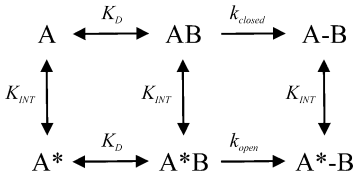

In this reaction mechanism, A and A* represent apo(a) in the closed and open conformations, respectively, and B represents LDL. AB and A*B represent noncovalent Lp(a) particles, while A−B and A*−B represent covalent Lp(a) particles. K_D is the dissociation constant for the interaction between apo(a) and LDL, K_{INT} is the intrinsic equilibrium constant between the open and closed conformations of apo(a), and k_{open} and k_{closed} are the rate constants for covalent Lp(a) particle formation for the open and closed conformations of apo(a), respectively. This model describes a scenario (see ref *21*) in which the conformational status of apo(a) influences the efficiency of covalent Lp(a) assembly by altering the rate constant for disulfide bond formation (k) and not the affinity of apo(a) for LDL (K_D). The rate equation for this reaction mechanism is displayed in eq 2 The general

$$\frac{V_0}{[A]_T} = \frac{[B]_T}{[B]_T + K_D}\left(\frac{k_{closed} + k_{open}K_{INT}}{1 + K_{INT}}\right) \quad (2)$$

form of eq 2 is a rectangular hyperbola given by

$$\frac{V_0}{[A]_T} = \frac{c[B]_T}{b + [B]_T} \quad (3)$$

where

$$b = K_D \quad (4)$$

$$c = \frac{k_{closed} + k_{open}K_{INT}}{1 + K_{INT}} \quad (5)$$

Scheme 2

$$A + B \overset{K_D}{\longleftrightarrow} AB \xrightarrow{k} A\text{-}B$$

Covalent Lp(a) assembly assays using varying concentrations of LDL were conducted to obtain K_D and K_{INT} from eqs 3−5. The rate constants for 17K r-apo(a), k_{open} and k_{closed}, were obtained previously (*21*).

Monitoring of the extent of covalent Lp(a) assembly over a period of 4 h was performed for the 17K, 12K, and 10K r-apo(a) variants. These assays were conducted at an LDL concentration of 50 nM using an identical procedure to the one described above with the exception that covalent Lp(a) formation was terminated at various time points (t = 0, 1, 2, 3, and 4 h). The extent of covalent Lp(a) particle formation [%Lp(a)] was determined and modeled as a function of time using an exponential rise to maximum equation shown below (Scheme 2).

Scheme 2 describes a reaction mechanism in which A represents apo(a) in the conformation that it adopts in the absence of ϵ-ACA [closed for 12K and 17K r-apo(a), open for 10K r-apo(a)] and B represents LDL. A−B and AB represent covalent and noncovalent Lp(a) complexes, respectively. K_D represents the dissociation constant for the noncovalent interaction between apo(a) and LDL, and k represents the rate constant for disulfide bond formation for apo(a) [k_{closed} for 12K and 17K r-apo(a), k_{open} for 10K r-apo(a)]. This model describes a scenario in which covalent Lp(a) assembly proceeds via a two-step process in which initial noncovalent interactions between apo(a) and LDL precede disulfide bond formation (*11*, *12*, *16*). Importantly, in the absence of ϵ-ACA, the vast majority of 17K and 12K r-apo(a) molecules adopt closed conformations. As such, Lp(a) formed from 12K or 17K r-apo(a) molecules in the open conformation need not be considered in kinetic analyses. Similarly, because 10K r-apo(a) adopts an open conformation in the absence of ϵ-ACA, covalent Lp(a) particles formed from this variant in the closed conformation need not be considered in kinetic analyses. Because we had independently measured the affinity of apo(a) for LDL (K_D) for each of the r-apo(a) derivatives, the rate constant k could be obtained from fitting the kinetic data according to eqs 6 and 7, where

$$\%\text{Lp(a)} = 100(1 - e^{-at}) \quad (6)$$

$$a = \frac{k[\text{B}]_T}{[\text{B}]_T + K_D} \quad (7)$$

RESULTS AND DISCUSSION

Closed Conformation of Apo(a) Is Maintained by an Intramolecular Interaction between Amino- and Carboxyl-Terminal Sequences. To identify sequences in apo(a) that maintain its closed conformation, we expressed recombinant proteins corresponding to the amino- (KIV_{1-4}) and carboxyl- (KIV_5-P) terminal halves of 17K r-apo(a) (Figure 1) and analyzed the physical properties of these proteins by intrinsic fluorescence. Titration of KIV_5-P or KIV_{1-4} with ϵ-ACA yielded fluorescence changes that were modeled according to simple hyperbolas to obtain dissociation constants (K_E) of 567.9 ± 41.4 μM and 41.0 ± 3.3 mM for the binding of ϵ-ACA to KIV_5-P or KIV_{1-4}, respectively (Figure 2A). As we have shown previously (*21*), 17K r-apo(a) undergoes a biphasic change in intrinsic fluorescence upon titration with ϵ-ACA; an increase in fluorescence is observed corresponding to a K_{E1} = 785 μM followed by a large decrease in fluorescence corresponding to a K_{E2} = 56.8 mM (Figure 2B). Interestingly, simultaneous titration of KIV_5-P and KIV_{1-4} with ϵ-ACA yielded fluorescence changes that did not precisely overlap with the profile obtained for 17K r-apo(a) (Figure 2B). When the intrinsic fluorescence profile for the simultaneous titration of KIV_5-P and KIV_{1-4} was subtracted from 17K, a hyperbolic decrease in fluorescence was obtained (inset of Figure 2B). Modeling of the additional fluorescence change in 17K according to a hyperbolic equation yielded a $K_{D(app)}$ value of 5.27 ± 1.15 mM and a maximal fractional fluorescence change of −0.0744 ± 0.0037. The affinity that characterizes this additional fluorescence change in 17K (K_D = 5.27 ± 1.15 mM) is in good agreement with the previously reported $K_{D(app)}$ value (8.05 ± 2.77 mM) for the binding of ϵ-ACA to the site(s) on apo-

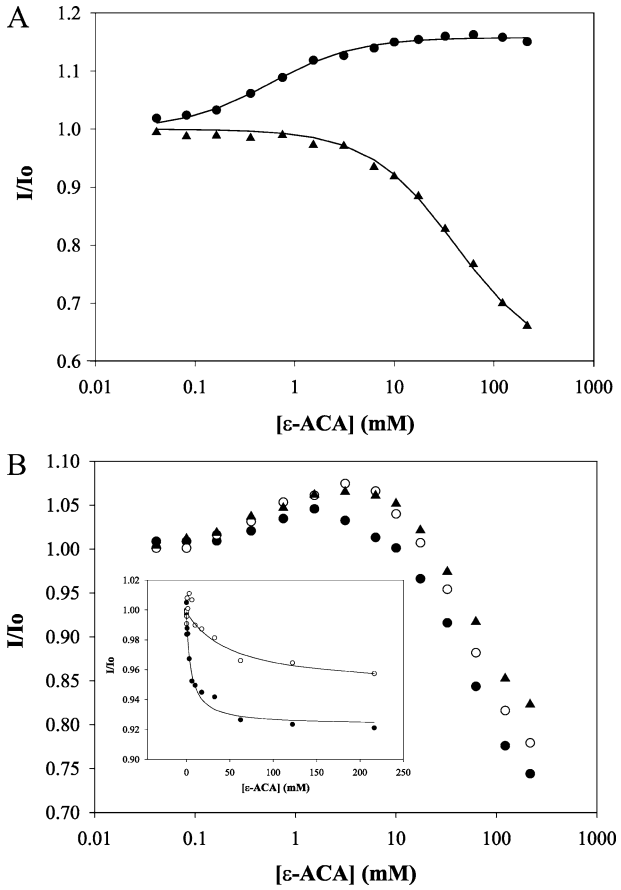

FIGURE 2: Effect of ϵ-ACA on the intrinsic fluorescence of apo(a). (A) KIV_{1-4} (▲) and KIV_5-P (●) (70 nM each) were titrated with ϵ-ACA, and the resultant changes in intrinsic fluorescence were recorded. The lines are a nonlinear regression of the data to hyperbolic equations representing the binding of ϵ-ACA to apo(a). (B) Identical intrinsic fluorescence experiments were performed using 17K (●), $17K_{KIV10}D56A$ (○), and KIV_{1-4} and KIV_5-P (▲) (70 nM each) simultaneously. (Inset) Fractional fluorescence changes (I/I_o) for either 17K (●) or $17K_{KIV10}D56A$ (○) were subtracted from the corresponding I/I_o values obtained for the simultaneous titration of KIV_{1-4} and KIV_5-P. The lines represent the fits obtained when the additional fluorescence changes observed for 17K (●) and $17K_{KIV10}D56A$ (○) were modeled to hyperbolic equations. The apparent dissociation constants [$K_{D(app)}$] obtained from the fits represent binding of ϵ-ACA to the site(s) on apo(a) that maintains its closed conformation.

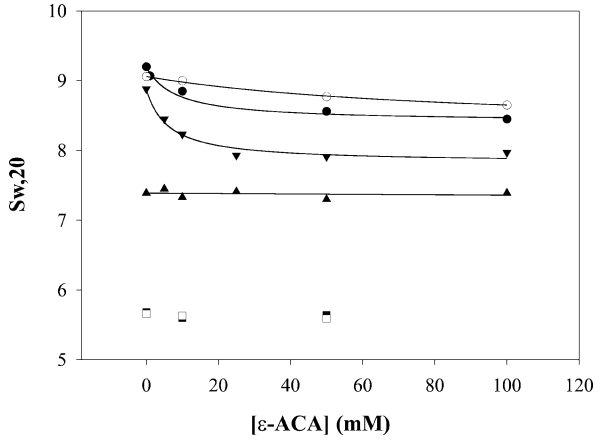

FIGURE 3: Effect of ϵ-ACA on the sedimentation coefficient of apo(a). Sedimentation coefficients for 17K (●), $17K_{KIV10}D56A$ (○), 12K (▼), 10K (▲), KIV_{1-4} (□), and KIV_5-P (■) in the presence of a wide range of ϵ-ACA concentrations were determined using AUC. The lines represent modeling of the data to either hyperbolic (17K, $17K_{KIV10}D56A$, and 12K) or linear (10K) equations. The data for 17K are from ref *21*.

(a) that maintains its closed conformation (*21*), suggesting that the closed conformation of apo(a) is maintained by an intramolecular interaction between sequences within the amino- and carboxyl-terminal halves of the molecule. To address this hypothesis, we assessed the effect of ϵ-ACA on the conformational status of apo(a) KIV_5-P and KIV_{1-4} using analytical ultracentifugation (AUC). The addition of ϵ-ACA had no effect on the sedimentation coefficients of either KIV_5-P or KIV_{1-4}, indicating that neither of these r-apo(a) variants adopt a closed conformation that can be converted to an open form upon binding to ϵ-ACA (Figure 3). When taken together, these data provide strong evidence for an interaction between sequences within the amino- and carboxyl-terminal halves of apo(a) that maintain its closed conformation; evidence for the interaction of these sequences in the closed conformation of apo(a) has also been suggested by electron microscopy (*27*). Interestingly, the closed conformation of plasminogen is also maintained by an interaction between sequences within the amino- and carboxyl-terminal halves of the protein; the amino-terminal tail domain of plasminogen interacts with kringle V in the closed conformation of the molecule (*28*). As is the case for apo(a), conversion of plasminogen to the open form is accompanied by changes in both the radius of gyration (*29*) and tryptophan fluorescence (*30*). However, apo(a) lacks an analogous tail domain to that which is present in plasminogen.

SLBS in Apo(a) KIV_{10} Is Involved in an Intramolecular Interaction with Amino-Terminal Sequences. Previous data from our laboratory suggest that the SLBS in apo(a) KIV_{10}, located within the carboxyl-terminal half of apo(a), is involved in maintaining the closed conformation of 17K (*21*). To substantiate this hypothesis, we used a 17K variant of apo(a) that contains a single amino acid substitution in the KIV_{10} SLBS ($17K_{KIV10}D56A$; Figure 1). The X-ray crystal structure of KIV_{10} predicts that this residue functions as a key part of the anionic center that coordinates the side-chain amino group of lysine (*31*). Surprisingly, mutating the SLBS in apo(a) KIV_{10} only modestly altered the conformational status of the protein as indicated by the minimal decrease in the sedimentation coefficient of $17K_{KIV10}D56A$ in the absence of ϵ-ACA ($S_{w,20} = 9.21$ for 17K (*21*) and 9.06 for $17K_{KIV10}$-D56A; see Figure 3). Interestingly, however, AUC data indicate that the amount of ϵ-ACA required to elicit the full conversion of $17K_{KIV10}D56A$ to the open conformation is considerably increased (~10-fold) compared to 17K, yielding a corresponding $K_{D(app)}$ value of 85.7 ± 11.3 mM (Figure 3). Intrinsic fluorescence experiments further substantiate this point. A comparison of the additional fluorescence changes (that report the transition from closed to open conformation; see above) obtained for the $17K_{KIV10}D56A$ and 17K variants reveals that there is a 10-fold reduction in the affinity ($17K_{KIV10}D56A$: $K_{D(app)} = 52.1$ mM; 17K: $K_{D(app)} = 5.27$ mM) and a 32% reduction in the maximal fractional fluorescence change ($17K_{KIV10}D56A$: $I/I_{o,max} = -0.0513$; 17K: $I/I_{o,max} = -0.0744$) that accompanies the conformational change for $17K_{KIV10}D56A$ (Figure 2B). A reduction in $I/I_{o,max}$ for $17K_{KIV10}D56A$ is consistent with this variant adopting a more open conformation in the absence of ϵ-ACA. These observations are in excellent agreement with AUC experiments, which demonstrate that, compared to 17K, the $17K_{KIV10}D56A$ variant adopts a slightly more open conformation in the absence of ϵ-ACA but requires 10-fold higher concentrations of this ligand to stimulate full conversion to the open form ($K_{D(app)} = 8.05$ mM for 17K, $K_{D(app)} = 85.7$ mM for $17K_{KIV10}D56A$) (Figure 3). When taken together, these data not only demonstrate that KIV_{10} is crucial in maintaining the closed conformation of apo(a), but also suggest that the D56A substitution in the SLBS in apo(a) KIV_{10} lowers the affinity of this kringle for ϵ-ACA to a much greater extent than for the sequences in apo(a) that maintain its closed conformation (i.e., internal ligand), suggesting that the internal ligand is *not* a lysine residue. The lysine-binding pocket of KIV_{10} can only accommodate one amino acid (*31*). As such, the observation that the addition of ϵ-ACA elicits a conformational change in apo(a) does not necessarily equate to ϵ-ACA competing with an internal lysine residue in apo(a) for binding to KIV_{10}. Thus, it becomes clear why a mutation (D56A) that diminishes the lysine-binding properties of KIV_{10} exhibits a modest effect on the conformation of apo(a).

The modest effect of the D56A mutation on the conformation of apo(a) translated into a markedly increased propensity (over 17K) of this derivative to form covalent Lp(a) particles (Figure 4A). To investigate whether this increased efficiency occurred at the level of noncovalent Lp(a) assembly or the rate of disulfide bond formation, we modeled the initial rate with which $17K_{KIV10}D56A$ forms covalent Lp(a) particles with respect to the concentration of LDL. Using eq 3 (described by Scheme 1), we obtained a K_D of 21.2 ± 8.6 nM for the noncovalent interaction between $17K_{KIV10}D56A$ and LDL and a constant (c) of 0.0835 ± 0.0119 h^{-1} that subsequently yielded a K_{INT} of 0.153 (see eq 5). These data clearly demonstrate that the increased rate of covalent Lp(a) particle formation observed for $17K_{KIV10}D56A$ is due to a 6-fold change in K_{INT} ($17K_{KIV10}D56A$: $K_{INT} = 0.153$; 17K: $K_{INT} = 0.025$; see ref *21*) and hence conformation, in the absence of an alteration of the affinity of $17K_{KIV10}D56A$ for LDL ($17K_{KIV10}D56A$: $K_D = 21.2 \pm 8.6$ nM; 17K: $K_D = 23.9 \pm 7.2$ nM; see ref *21*). The lack of an effect on the noncovalent step of Lp(a) assembly was corroborated experimentally by titrating flu-LDL with $17K_{KIV10}D56A$,

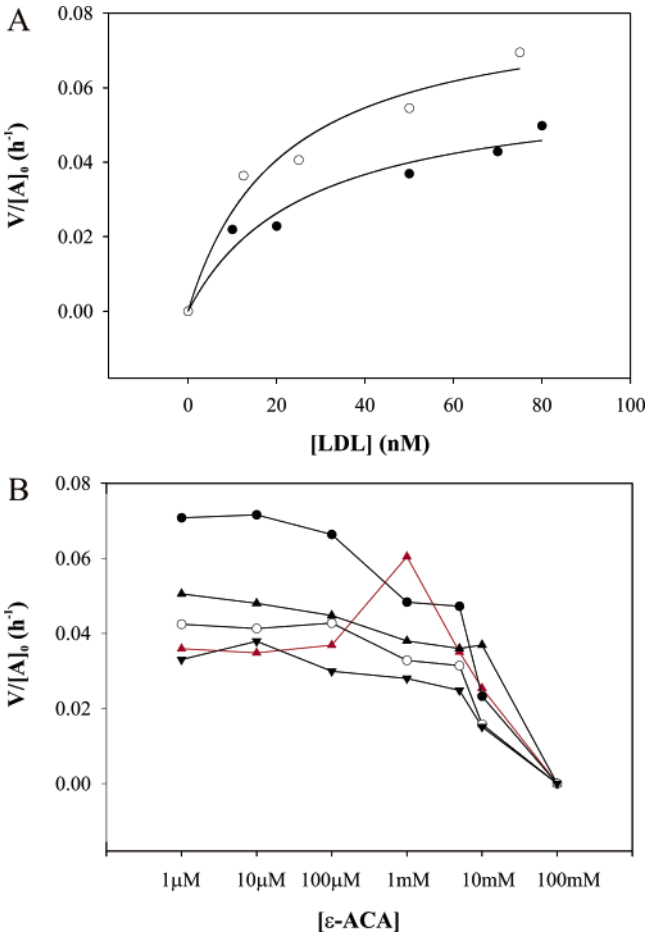

FIGURE 4: Effect of the D56A mutation in apo(a) KIV_{10} on covalent Lp(a) assembly. (A) Velocity of covalent Lp(a) particle assembly for $17K_{KIV10}D56A$ (○) and 17K (●) (the latter taken from ref *21*) in the absence of ϵ-ACA was measured at various concentrations of LDL. A hyperbolic relationship described by eqs 3−5, was derived from first principles based on the model shown in Scheme 1. The lines represent the fit obtained upon subjecting the data to a nonlinear regression using eq 3, yielding a K_D for the noncovalent interaction between LDL and apo(a) and a constant *a*. (B) In vitro covalent Lp(a) assembly assays using metabolically labeled $17K_{KIV10}$-D56A (4 nM) and a variety of LDL concentrations (12.5 nM, ▼; 25 nM, ○; 50 nM, ▲; 75 nM, ●) were conducted in the presence of increasing concentrations of ϵ-ACA (0−100 mM). The fraction of apo(a) present as covalent Lp(a) particles was determined by SDS−PAGE followed by fluorography and densitometric analysis. The velocity of covalent Lp(a) particle formation (*V*) was calculated by dividing the amount of Lp(a) formed (in nanomolars) by the end of the reaction (4 h) and by the duration of the reaction. For a comparison, the initial rate of covalent Lp(a) particle formation using 4 nM 17K and 50 nM LDL at various concentrations of ϵ-ACA (red triangles, red line) is presented (see ref *21*).

which yielded a K_D of 31.5 ± 8.8 nM compared to 23.9 ± 7.2 nM for 17K (*21*) (Table 1).

On a molecular level, the 6-fold change in K_{INT} reflects a 6-fold reduction in the affinity of KIV_{10} for the internal ligand resulting from the D56A mutation. Furthermore, the K_{INT} and $K_{D(app)}$ values for 17K and $17K_{KIV10}D56A$ can be used to quantify the effect of the D56A mutation on the affinity (K_E) of KIV_{10} for ϵ-ACA (i.e., $K_{D(app)} = K_E/K_{INT}$). The results of this analysis demonstrate a 60-fold reduction in the affinity of $KIV_{10}D56A$ (versus KIV_{10}) for ϵ-ACA. When taken together, these data provide quantitative experimental evidence for our hypothesis that the D56A mutation affects

Table 1: Analysis of Noncovalent Binding between Recombinant Apo(a) Variants and flu-LDL

r-apo(a) variant[a]	K_D (nM)[b]
17K	23.9 ± 7.2[c]
$17K_{KIV10}D56A$	31.5 ± 8.8
12K	34.7 ± 2.2
10K	26.0 ± 8.8

[a] r-apo(a) variants are shown schematically in Figure 1. [b] K_D values were determined using a solution-phase, fluorescence-based binding assay in which LDL was labeled with 5′-iodoacetamido-fluorescein. Values reported for K_D are representative of three independent experiments. [c] From ref *21*.

binding to ϵ-ACA to a greater extent than to the internal ligand. Clearly, the identification of sequences in apo(a) that interact with KIV_{10} in the closed conformation will be required to rationally design site-directed mutations in KIV_{10} that more potently affect internal ligand binding in the closed conformation of the molecule.

We have previously reported that the addition of ϵ-ACA elicits a biphasic effect on the initial rate of covalent Lp(a) particle formation for 17K; low concentrations of ϵ-ACA enhance the process by altering the conformational status of apo(a), while higher concentrations of this ligand potently attenuate the process by inhibiting noncovalent interactions between apo(a) and LDL (*21*). Unlike that observed for 17K r-apo(a), the addition of ϵ-ACA did not elicit a biphasic effect on the initial rate of covalent Lp(a) assembly using the $17K_{KIV10}D56A$ variant, which resulted in a simple inhibitory profile (Figure 4B). This result is in keeping with our observation that the D56A mutation in KIV_{10} drastically reduces (∼60-fold) the affinity of this domain for ϵ-ACA; the amount of ϵ-ACA required to elicit the conformational change in the $17K_{KIV10}D56A$ variant is elevated ($K_{D(app)}$ = 85.7 mM) to concentrations high enough to completely abolish initial noncovalent binding to LDL. Thus, while the minimal change in K_{INT} (i.e., conformation) exerts only a mild effect on the rate of covalent Lp(a) assembly in the absence of ϵ-ACA, the large change in K_E (i.e., affinity for ϵ-ACA) completely abrogates the biphasic effect of ϵ-ACA on the initial rate of covalent Lp(a) particle formation (Figure 4B). These data underscore the important role played by KIV_{10} in maintaining the closed conformation of apo(a).

Apo(a) Isoform Size Affects the Conformation of Apo(a). The closed conformation of apo(a) is associated with a decreased rate of covalent Lp(a) assembly, possibly by restricting access of LDL to the free sulfhydryl group in apo(a) KIV_9. As previously stated, apo(a) exhibits marked isoform size heterogeneity within the human population (*6*, *7*). Using differently sized recombinant apo(a) isoforms, we investigated the effect of apo(a) isoform size heterogeneity on the conformation of apo(a), as well as on the efficiency of both noncovalent and covalent Lp(a) assembly. The 12K r-apo(a) variant (containing 3 KIV_2 domains) exhibited an ϵ-ACA-induced conformational change from a closed to open form as indicated by the nonlinear decrease in $S_{w,20}$ observed for this variant in AUC experiments (Figure 3). Moreover, the $K_{D(app)}$ value for the 12K r-apo(a) (6 ± 1 mM) variant is in good agreement with that previously reported for the 17K r-apo(a) variant ($K_{D(app)}$ = 8.03 ± mM; ref *21*) indicating that reducing the KIV_2 copy number from eight (in 17K) to three (in 12K) does not alter the conformational status of

apo(a). Interestingly, an ϵ-ACA-induced conformational change in the 10K r-apo(a) variant (containing one KIV_2 domain) was not observed, as indicated by the absence of a change in the sedimentation coefficient for this variant in the presence of ϵ-ACA (Figure 3). It appears that greater than one copy of KIV_2 must be present for apo(a) to adopt a closed conformation. Electron microscopy studies of apo(a) have described a structure that resembles "beads on string", with rigid kringle domains connected by flexible interkringle sequences (*27*). Because KIV_2 is present in 10K r-apo(a), which adopts an open conformation, it is unlikely that this domain directly participates in an intramolecular interaction with the SLBS in KIV_{10}. It is possible, however, that more than one copy of KIV_2 is required to provide enough length and flexibility (because of the presence of extra interkringle sequences) to enable an intramolecular interaction between the amino-terminal half of apo(a) and sequences within KIV_{10}.

Apo(a) Isoform Size Is Inversely Proportional to the Efficiency of Covalent Lp(a) Assembly. Having demonstrated that the number of KIV_2 domains in apo(a) affects the conformational status of the protein, we next investigated the ability of differently sized isoforms of apo(a) to form both noncovalent and covalent Lp(a) particles. Titration of flu-LDL with either 10K or 12K r-apo(a) yielded nonlinear decreases in fluorescence that were subsequently modeled according to eq 1, yielding K_D values of 34.7 $\pm$ 2.2 nM and 26.0 $\pm$ 8.8 nM for the 12K and 10K r-apo(a) variants, respectively (Table 1). The K_D for the interaction between 17K r-apo(a) and flu-LDL was previously determined to be 23.9 $\pm$ 7.2 nM (*21*), indicating that apo(a) isoform size does not affect its affinity for LDL.

Although apo(a) isoform size did not alter the affinity of apo(a) for LDL, it exerted a profound effect on the initial rate of covalent Lp(a) particle formation. Titration with ϵ-ACA resulted in a biphasic effect on the initial rate of covalent Lp(a) particle formation using the 12K r-apo(a) variant (Figure 5A). This biphasic relationship is consistent with the notion that the 12K r-apo(a) variant undergoes an ϵ-ACA-induced conformational change from a closed to open form. As we have previously shown with 17K r-apo(a) (*21*), the magnitude of the ϵ-ACA-mediated enhancement is sensitive to the ratio of LDL/apo(a) because higher concentrations of LDL partly alleviate inhibition of the noncovalent step of Lp(a) assembly by ϵ-ACA (Figure 5A). In contrast to the 12K and 17K r-apo(a) variants, a biphasic relationship was not observed for the 10K variant (Figure 5B). This observation is consistent with AUC data, which indicate that this r-apo(a) variant adopts an open conformation in the absence of ϵ-ACA (Figure 3).

The efficiency of covalent Lp(a) assembly in the absence of ϵ-ACA is inversely correlated with apo(a) isoform size. Because altering apo(a) isoform size did not affect the solution-phase affinity of apo(a) for LDL (Table 1), variations in the efficiency of covalent Lp(a) assembly must be accounted for by alterations in the rate constant (k) for disulfide bond formation between the various apo(a) variants and LDL. To further investigate this relationship, we performed covalent Lp(a) assembly assays using 17K, 12K, and 10K r-apo(a) variants over a time course of 4 h (Figure 5C). The inverse relationship between apo(a) isoform size and the rate of covalent Lp(a) particle formation is clearly

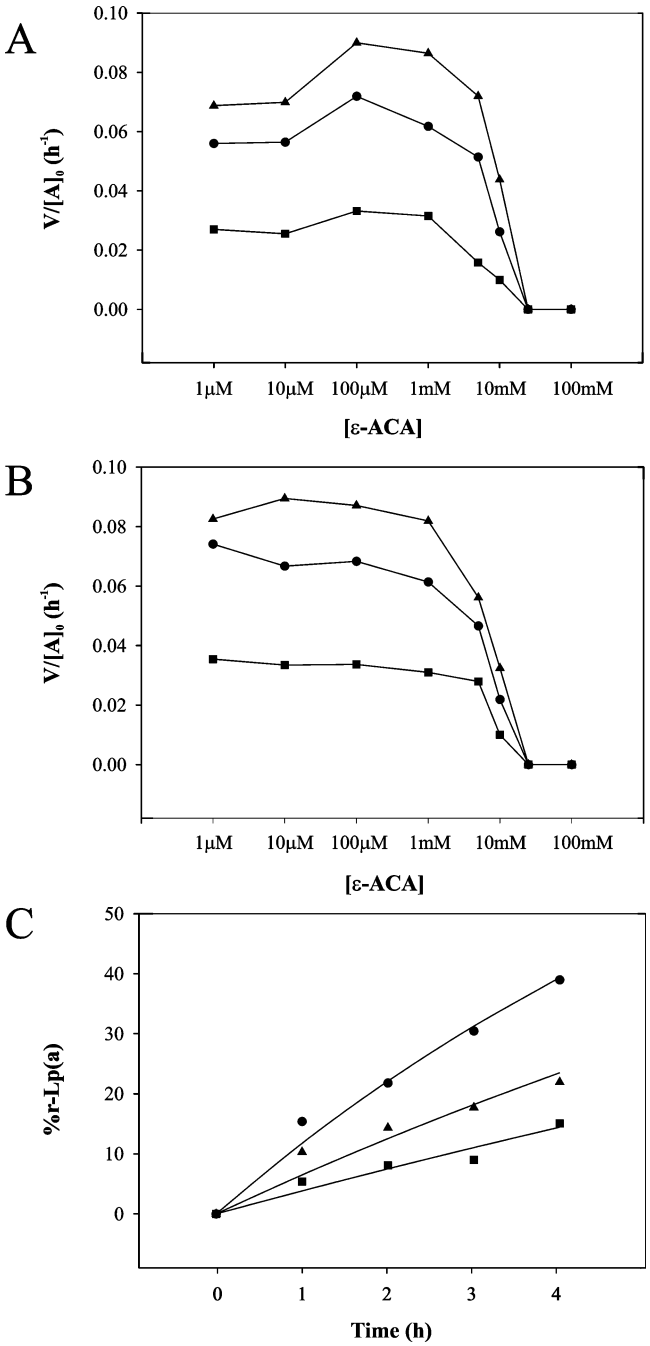

FIGURE 5: Effect of apo(a) isoform size heterogeneity on covalent Lp(a) assembly. In vitro covalent Lp(a) assembly assays, using metabolically labeled 12K (A) and 10K (B) were conducted with different concentrations of LDL (12.5 nM, ■; 25 nM, ●; and 50 nM, ▲) in the presence of a range of ϵ-ACA concentrations (0−100 mM) at 37 °C for 4 h. The data were treated in the same manner as those for the $17K_{KIV10}D56A$ variant (see Figure 4B). (C) In vitro covalent Lp(a) assembly assays using metabolically labeled 17K (■), 12K (▲), or 10K (●) (4 nM) and LDL (50 nM) were conducted at 37 °C for variable times (t = 0, 1, 2, 3, or 4 h). The lines represent a regression of the data according to eq 6.

demonstrated over the entire time course. Modeling of the data using eq 6 yielded a constant (a) that incorporates the rate constant for covalent Lp(a) assembly (k), the total concentration of LDL ($[B]_0$), and the affinity of apo(a) for LDL (K_D) (see eq 7) for each r-apo(a) variant: $a = 0.039 \pm 0.003$ h^{-1} for 17K, $a = 0.067 \pm 0.005$ h^{-1} for 12K, and $a = 0.125 \pm 0.005$ h^{-1} for 10K. Using eq 7, we obtained the following rate constants: $k = 0.0576$ h^{-1} for 17K, $k = 0.113$

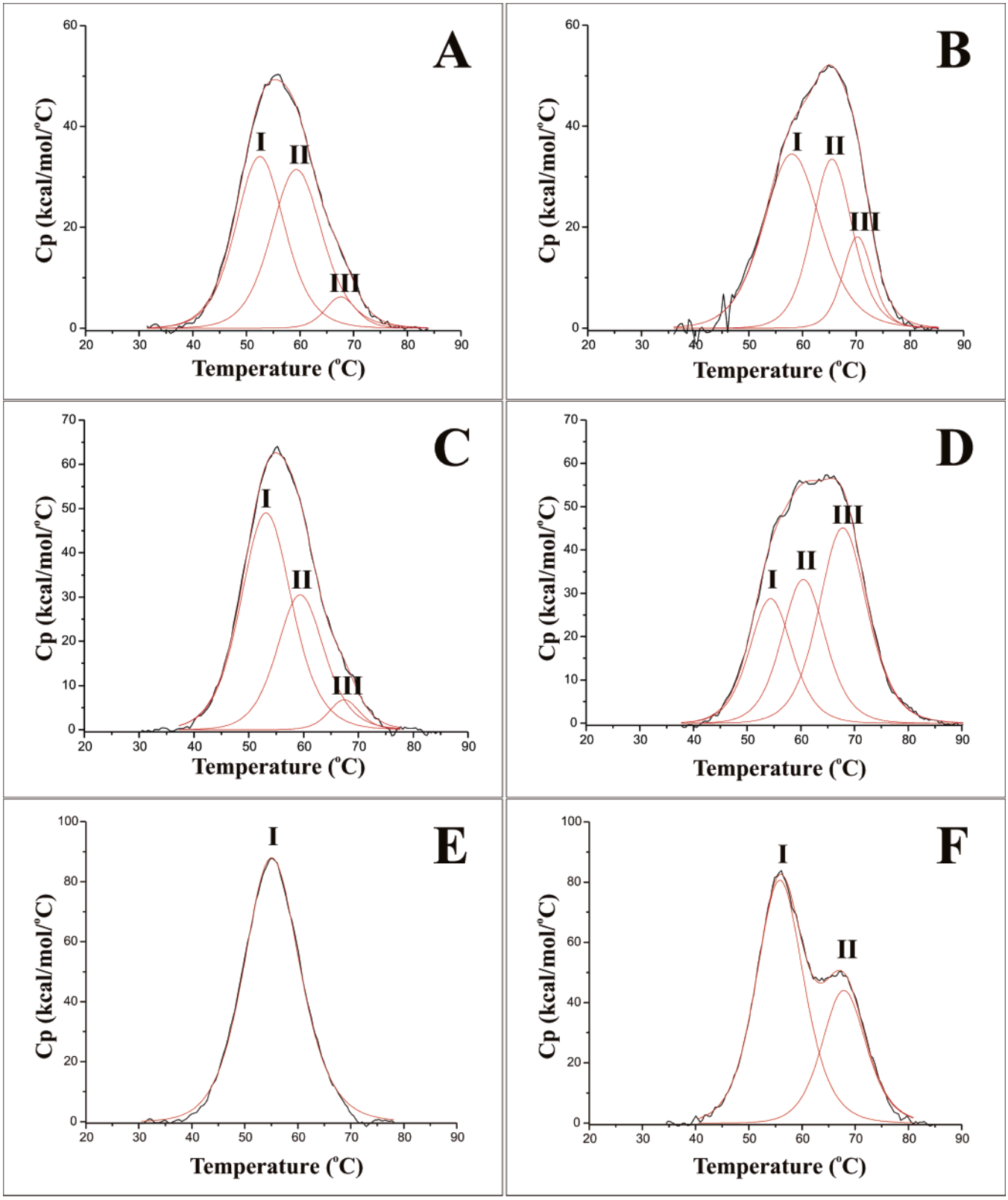

FIGURE 6: DSC of 10K and 12K recombinant apo(a) in the presence of ϵ-ACA. The corrected thermal denaturation profiles were modeled according to a non-two-state model that describes three independent thermal transitions. The red lines correspond to the fits obtained to the data (black lines). (A and B) 10K r-apo(a) in the presence of 0 and 50 mM ϵ-ACA, respectively. (C and D) 12K r-apo(a) in the presence of 0 and 50 mM ϵ-ACA, respectively. (E and F) 17K r-apo(a) in the presence of 0 and 50 mM ϵ-ACA, respectively. The data for 17K are from ref *21*.

h^{-1} for 12K, and $k = 0.200\ h^{-1}$ for 10K. The rate constant observed for 17K ($k = 0.0576\ h^{-1}$) is in good agreement with the previously determined rate constant for the closed conformation of 17K ($k_{closed} = 0.0497\ h^{-1}$) (*21*). Because 10K adopts an open conformation, it follows that this variant has an increased propensity to form covalent Lp(a) particles. In fact, the observed rate constant for 10K ($k = 0.200\ h^{-1}$) is reasonably consistent with the rate constant previously

Table 2: Analysis of the Thermal Denaturation of Apo(a) in the Absence of ϵ-ACA

parameter	17K r-apo(a)[a]	12K r-apo(a)	10K r-apo(a)
T_{mI} (°C)	55.2	53.3	53.8
ΔH_{mI} (kcal mol^{-1})	1.2×10^6	6.0×10^5	4.0×10^5
ΔH^*_{mI} (kcal mol^{-1})	6.2×10^4	6.9×10^4	7.2×10^4
$\Delta H_{mI}/\Delta H^*_{mI}$	19.4	8.70	5.56
T_{mII} (°C)	NA[b]	59.5	59.3
ΔH_{mII} (kcal mol^{-1})	NA	3.4×10^5	3.3×10^5
ΔH^*_{mII} (kcal mol^{-1})	NA	7.7×10^4	7.3×10^4
$\Delta H_{mII}/\Delta H^*_{mII}$	NA	4.42	4.52
T_{mIII} (°C)	NA	67.5	67.4
ΔH_{mIII} (kcal mol^{-1})	NA	5×10^4	8.4×10^4
ΔH^*_{mIII} (kcal mol^{-1})	NA	1.3×10^5	9.8×10^5
$\Delta H_{mIII}/\Delta H^*_{mIII}$	NA	0.38	0.85

[a] From ref *21*. [b] NA = not applicable.

reported for the open conformation of 17K r-apo(a) (k_{open} = 0.304 h^{-1}) (*21*).

The 12K r-apo(a) variant, however, adopts a closed conformation, and thus it is more difficult to account for the increased ability of this variant to form covalent Lp(a) particles compared to 17K. Given that the $K_{D(app)}$ values for 17K and 12K are nearly identical, it is highly unlikely that an increased K_{INT} value and hence an increased proportion of molecules in the open conformation accounts for the increased efficiency of covalent Lp(a) formation observed with 12K. Another hypothesis to explain this observation is that the closed conformation of 12K is less inhibitory to covalent Lp(a) assembly than the closed conformation of 17K. This would be consistent with the notion that the closed conformation of apo(a) inhibits covalent Lp(a) assembly by restricting access of LDL to the free cysteine in apo(a) KIV_9. In this regard, reducing the KIV_2 copy number from eight (17K) to three (12K) may alleviate steric hindrance imposed by the amino-terminal half of apo(a), thereby resulting in an enhancement of the rate of covalent Lp(a) assembly for 12K. To test this hypothesis, we compared the physical properties of 10K, 12K, and 17K in the presence and absence of ϵ-ACA using DSC.

DSC as a Measure of the Conformational Status of Apo(a) Isoforms. We have previously determined that in DSC experiments, 17K r-apo(a) undergoes a single thermal transition that is characterized by the presence of 19 domains and a melting temperature (T_m) of 55.2 °C, which is suggestive of interdomain interactions within this molecule (*21*). Addition of ϵ-ACA resulted in a dose-dependent appearance of a second thermal transition in 17K that, at saturation, is characterized by the presence of 5−6 domains with a T_m of 69 °C (*21*). The thermal denaturation of 10K, which did not undergo an ϵ-ACA-induced conformational change, was characterized by the presence of three distinct thermal transitions in the absence of ϵ-ACA (Figure 6A). Modeling of the thermal denaturation of 10K according to a non-two-state model yielded a T_m and temperature-independent van't Hoff and calorimetric heat changes (ΔH_m and ΔH^*_m, respectively) for each transition (Table 2). Importantly, the ratio of $\Delta H_m/\Delta H^*_m$ represents the number of structural units undergoing a particular thermal transition (*32*). The addition of ϵ-ACA did not elicit a conformational change in 10K as indicated by the absence of a transfer of domains from one thermal transition to another (parts A and B of Figure 6 and Figure 7A). The denaturation profile of

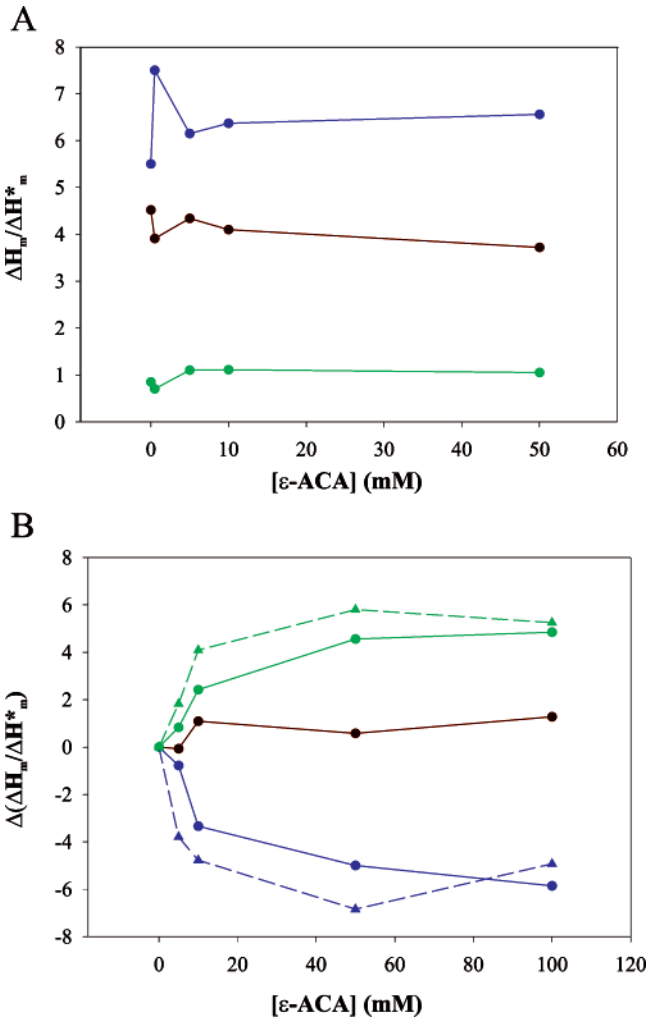

FIGURE 7: Measurement of the conformational status of apo(a) by DSC. The temperature-independent calorimetric (ΔH_m) and van't Hoff (ΔH^*_m) heat changes were obtained for each thermal transition at each concentration of ϵ-ACA by modeling the data from Figure 6 according to a non-two-state-model. The change in the ratio of $\Delta H_m/\Delta H^*_m$ [$\Delta(\Delta H_m/\Delta H^*_m)$] at each thermal transition was plotted with respect to the concentration of ϵ-ACA. (A) Data obtained for Peaks I (blue), II (red), and III (green) for 10K r-apo(a). (B) Data obtained for Peaks I (blue circles, solid line), II (red circles, solid line), and III (green circles, solid line) for 12K r-apo(a) and for Peaks I (blue triangles, dashed line) and II (green triangles, dashed line) for 17K r-apo(a). The data obtained for the 17K r-apo(a) variant are from ref *21*.

12K is also characterized by three distinct thermal transitions (Figure 6C and Table 2). Although 12K adopts a closed conformation, the denaturation profile of this variant in the absence of ϵ-ACA is very similar to 10K in that three thermal transitions are observed. This suggests that the closed conformation of 12K is less restrictive than that for 17K because the additional peaks (in the absence of ϵ-ACA) indicate a decreased extent of interdomain interactions in 12K. Unlike the 10K variant, titration of 12K with ϵ-ACA resulted in a dose-dependent movement of ~5 domains from peak I (T_m = 53.3 °C) to peak III (T_m = 69 °C) (parts C and D of Figure 6 and Figure 7B); the same phenomenon was previously observed for 17K (*21*). When the movement of the domains in 12K was modeled with respect to the concentration of ϵ-ACA, a $K_{D(app)}$ value of 15 ± 3 mM was obtained. A comparison of this value with that obtained (Figure 7B) for 12K in AUC experiments ($K_{D(app)}$ = 6 mM)

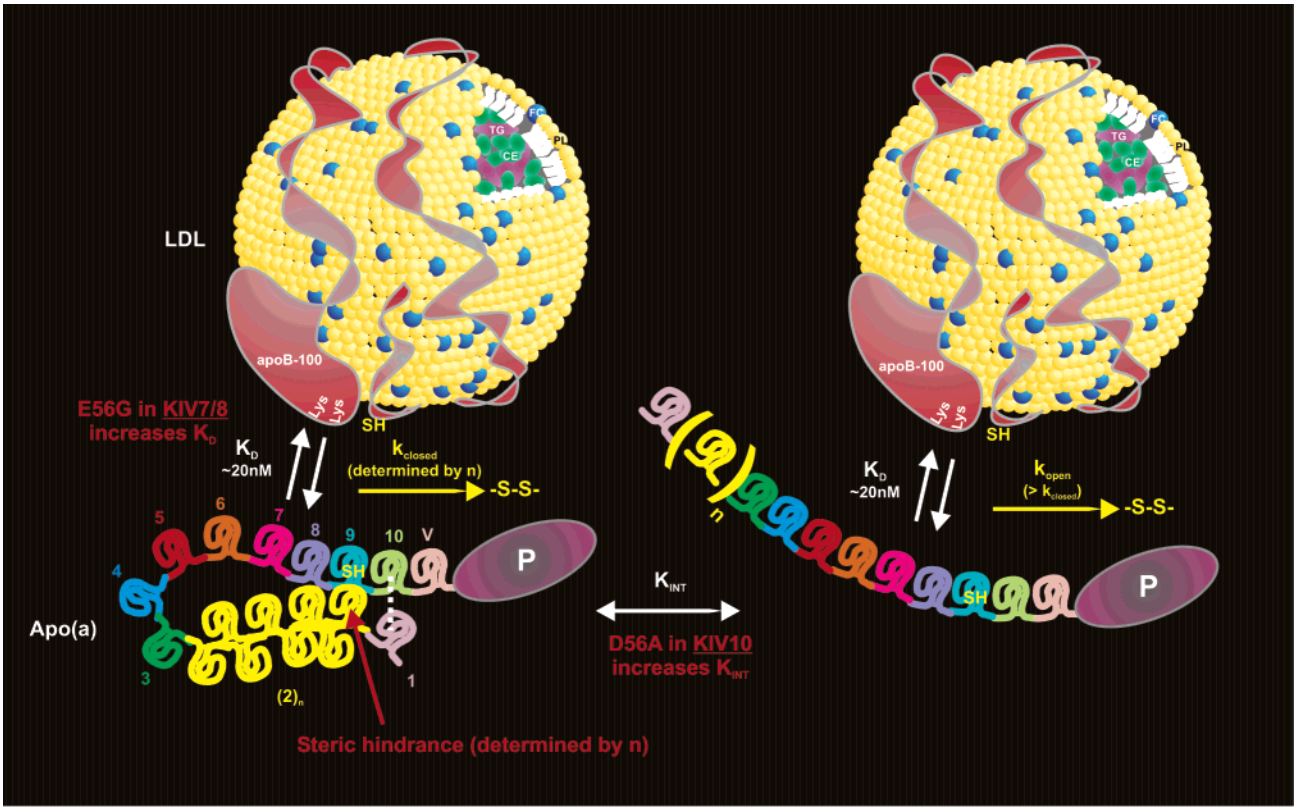

FIGURE 8: Integrative model for Lp(a) assembly. On the basis of the present study, as well as previous work from our laboratory (see refs *18*, *20*, *21*), a model for Lp(a) assembly is shown that demonstrates regulation at the level of both the noncovalent and covalent steps of the process. Please refer to the text for details. We have depicted the intramolecular interaction between KIV_1 and KIV_{10} for convenience.

indicates that, as for 17K (*21*), DSC is reporting the conformational change in 12K.

Determination of the Efficiency of Covalent Lp(a) Particle Formation. An integrative model for Lp(a) assembly is presented (Figure 8) based on the findings reported in this manuscript as well as previous work from our laboratory. Because Lp(a) assembly occurs as a two-step process, the rate of covalent Lp(a) particle formation is determined both by the affinity of apo(a) for LDL (K_D) as well as by the rate constant (k) for disulfide bond formation. A recent study by our group demonstrated that the WLBSs within apo(a) KIV_{7-8} mediate noncovalent binding to LDL but are not involved in maintaining the closed conformation of apo(a) (*18*). Accordingly, mutation of these domains decreases the efficiency of covalent Lp(a) particle formation by altering the K_D for the noncovalent interaction between apo(a) and LDL. In contrast, the present study clearly shows that the conformational status of apo(a) influences the rate of covalent Lp(a) assembly at the level of k and not K_D. We demonstrate here that the conformational status of apo(a) can be influenced by performing mutagenesis on the SLBS in KIV_{10}, thereby increasing the proportion of apo(a) molecules in the open versus closed form (K_{INT}), while the extent of inhibition (k_{closed}) imposed by the closed conformation of apo(a) is regulated by the number of KIV_2 repeats. Modulation of the efficiency of Lp(a) assembly in vivo could potentially be mediated by regulation of the noncovalent and/or covalent steps of the process. To highlight this point, our demonstration that apo(a) isoform size is inversely correlated with the rate constant for the covalent step of Lp(a) assembly may, in part, explain the inverse relationship between apo(a) isoform size and plasma concentrations of apo(a) that has been observed within the human population (*9*).

ACKNOWLEDGMENT

The authors wish to thank the Protein Function Discovery Group at Queen's University for subsidizing the use of the analytical ultracentrifuge and calorimeter.

REFERENCES

1. Marcovina, M., Koschinsky, M. L., Albers, J. J., and Skarlatos, S. (2003) Report of the National Heart, Lung, and Blood Institute workshop on lipoprotein(a) and cardiovascular disease: Recent advances and future directions, *Clin. Chem. 49*, 1785−1796.
2. Marcovina, S. M., and Koschinsky, M. L. (2003) Evaluation of lipoprotein(a) as a prothrombotic factor: Progress from bench to bedside, *Curr. Opin. Lipidol. 14*, 361−366.
3. . Koschinsky, M. L., Côté, G., Gabel, B., and van der Hoek, Y. Y. (1993) Identification of the cysteine residue in apolipoprotein-(a) that mediates extracellular coupling with apolipoprotein B-100, *J. Biol. Chem. 268*, 19819−19825.
4. Brunner, C., Kraft, H.-G., Utermann, G., and Müller, H.-J. (1993) Cys4057 of apolipoprotein(a) is essential for lipoprotein(a) assembly, *Proc. Natl. Acad. Sci. U.S.A. 90*, 11643−11647.
5. McLean, J. W., Tomlinson, J. E., Kuang, W.-H., Eaton, D. L., Chen, E. Y., Fless, G. M., Scanu, A. M., and Lawn, R. M. (1987) cDNA sequence of human apolipoprotein(a) is homologous to plasminogen, *Nature 330*, 132−137.
6. Lackner, C., Cohen, J. C., and Hobbs, H. H. (1993) Molecular definition of the extreme size polymorphism in apolipoprotein-(a), *Hum. Mol. Genet. 2*, 933−940.
7. van der Hoek, Y. Y., Wittekoek, M. E., Beisiegel, U., Kastelein, J. J. P., and Koschinsky, M. L. (1993) The apolipoprotein(a) kringle IV repeats which differ from the major repeat kringle are present in variably sized isoforms, *Hum. Mol. Genet. 2*, 361−366.

8. Marcovina, S. M., Hobbs, H. H., and Albers, J. J. (1996) Relation between number of apolipoprotein(a) kringle 4 repeats and mobility of isoforms in agarose gel: Basis for a standardized isoform nomenclature, *Clin. Chem. 42*, 436−439.
9. Utermann, G., Kraft, H. G., Menzel, H. J., Hopferwieser, T., and Seitz, C. (1988) Genetics of the quantitative Lp(a) lipoprotein trait. I. Relation of LP(a) glycoprotein phenotypes to Lp(a) lipoprotein concentrations in plasma, *Hum. Genet. 78*, 41−46.
10. Brunner, C., Lobentanz, E. M., Petho-Schramm, A., Ernst, A., Kang, C., Dieplinger, H., Muller, H. J., and Utermann, G. (1996) The number of identical kringle IV repeats in apolipoprotein(a) affects its processing and secretion by HepG2 cells, *J. Biol. Chem. 271*, 32403−32410.
11. Ernst, A., Helmhold, M., Brunner, C., Petho-Schramm, P., Armstrong, V. W., and Müller, H.-J. (1995) Identification of two functionally distinct lysine-binding sites in kringle 37 and in kringles 32−36 of human apolipoprotein(a), *J. Biol. Chem. 270*, 6227−6234.
12. Gabel, B. R., May. L. F., Marcovina, S. M., and Koschinsky, M. L. (1996) Lipoprotein(a) assembly. Quantitative assessment of the role of apo(a) kringle IV types 2−10 in particle formation. *Arterioscler., Thromb., Vasc. Biol. 16*, 1559−1567.
13. Sangrar, W., Marcovina, S. M. and Koschinsky, M. L. (1994) Expression and characterization of apolipoprotein(a) kringle IV types 1, 2, and 10 in mammalian cells, *Protein Eng. 7*, 723−731.
14. Harpel, P. C., Gordon, B. R., and Parker, T. S. (1989) Plasmin catalyzes binding of lipoprotein(a) to immobilized fibrinogen and fibrin, *Proc. Natl. Acad. Sci. U.S.A. 86*, 3847−3851.
15. LoGrasso, P. V., Cornell-Kennon, S., and Boettcher, B. R. (1994) Cloning, expression, and characterization of human apolipoprotein-(a) kringle IV37, *J. Biol. Chem. 269*, 21820−21827.
16. Trieu, V. N., and McConathy, W. J. (1995) A two-step model for lipoprotein(a) formation, *J. Biol. Chem. 270*, 15471−15474.
17. Gabel, B. R., and Koschinsky, M. L. (1998) Sequences within apolipoprotein(a) kringle IV types 6−8 bind directly to low-density lipoprotein and mediate noncovalent association of apolipoprotein-(a) with apolipoprotein B-100, *Biochemistry 37*, 7892−7898.
18. Becker, L., Cook, P. M., Wright, T. G., and Koschinsky, M. L. (2004) Quantitative evaluation of the contribution of weak lysine-binding sites present within apolipoprotein(a) kringle IV types 6−8 to lipoprotein(a) assembly, *J. Biol. Chem. 279*, 2679−2688.
19. Gabel, B. R., McLeod, R. S., Yao, Z., and Koschinsky, M. L. (1998) Sequences within the amino terminus of ApoB100 mediate its noncovalent association with apo(a), *Arterioscler., Thromb., Vasc. Biol. 18*, 1738−1744.
20. Becker, L., McLeod, R. S., Marcovina, S. M., Yao, Z., and Koschinsky, M. L. (2001) Identification of a critical lysine residue in apolipoprotein B-100 that mediates noncovalent interaction with apolipoprotein(a), *J. Biol. Chem. 276*, 36155−36162.
21. Becker, L., Webb, B. A., Chitayat, S., Nesheim, M. E., and Koschinsky, M. L. (2003) A ligand-induced conformational change in apolipoprotein(a) enhances covalent Lp(a) formation, *J. Biol. Chem. 278*, 14074−14081.
22. Koschinsky, M. L., Tomlinson, J. E., Zioncheck, T. F., Schwartz, K., Eaton, D. L., and Lawn, R. M. (1991) Apolipoprotein(a): Expression and characterization of a recombinant form of the protein in mammalian cells, *Biochemistry 30*, 5044−5051.
23. Sangrar, W., Gabel, B. R., Boffa, M. B., Walker, J. B., Hancock, M. A., Marcovina, S. M., Horrevoets, A. J. G., Nesheim, M. E., and Koschinsky, M. L. (1997) The solution phase interaction between apolipoprotein(a) and plasminogen inhibits the binding of plasminogen to a plasmin-modified fibrinogen surface, *Biochemistry 36*, 10353−10363.
24. Hancock, M. A., Boffa, M. B., Marcovina, S. M., Nesheim, M. E., and Koschinsky, M. L. (2003) Inhibition of plasminogen activation by lipoprotein(a): Critical domains in apolipoprotein-(a) and mechanism of inhibition on fibrin and degraded fibrin surfaces, *J. Biol. Chem. 278*, 23260−23269.
25. Fodor, S. P. A., Copeland, R. A., Grygon, C. A., and Spiro, T. G. (1989) Deep-ultraviolet Raman excitation profiles and vibronic scattering mechanisms of phenylalanine, tyrosine, and tryptophan, *J. Am. Chem. Soc. 111*, 5509−5518.
26. Laemmli, U. K. (1970) Cleavage of structural proteins during the assembly of the head of bacteriophage T4, *Nature 227*, 680−685.
27. Weisel, J. W., Nagaswami, C., Woodhead, J. L., Higazi, A. A., Cain, W. J., Marcovina, S. M., Koschinsky, M. L., Cines, D. B., and Bdeir, K. (2001) The structure of lipoprotein(a) and ligand-induced conformational changes, *Biochemistry 40*, 10424−10435.
28. Cockell, C. S., Marshall, J. M., Dawson, K. M., Cederholm-Williams, S. A., and Ponting, C. P. (1998) Evidence that the conformation of unliganded human plasminogen is maintained via an intramolecular interaction between the lysine-binding site of kringle 5 and the N-terminal peptide, *Biochem. J. 333*, 99−105.
29. Kornblatt, J. A. (2000) Understanding the fluorescence changes of human plasminogen when it binds the ligand, 6-aminohexanoate: A synthesis, *Biochim. Biophys. Acta 1481*, 1−10.
30. Mangel, W. F., Lin, B. H., and Ramakrishnan, V. (1990) Characterization of an extremely large, ligand-induced conformational change in plasminogen, *Science 248*, 69−73.
31. Mikol, V., LoGrasso, P. V., and Boettcher, B. R. (1996) Crystal structures of apolipoprotein(a) kringle IV37 free and complexed with 6-aminohexanoic acid and with *p*-aminomethylbenzoic acid: Existence of novel and expected binding modes, *J. Mol. Biol. 8*, 751−761.
32. Privalov, P. L., and Potekhin, S. A. (1986) Scanning microcalorimetry in studying temperature-induced changes in proteins, *Methods Enzymol. 131*, 4−51.

BI049536D